Proceedings, 7th African Rift Geothermal Conference
Kigali, Rwanda 31st October – 2nd November 2018

The Crustal Structure of Northern Kenya Rift: Results from micro Earthquakes Data <Title Style>

Deflorah kangogo, Peter Kamau,John Kiama, Robert Mukiri and Teresia Nguuri Francis

Geothermal Development Company (GDC), Kenyatta Ave. Generation Building,

P.O. Box: 17700-20100, Nakuru, Kenya

dkangogo@gdc.co.ke; pkamau@gdc.co.ke; rmukiri@gdc.co.ke;;tnguurifrancis@gdc.co.ke.

Key words: *Crustal structure, Double Difference (Hypo DD), Velocity model,*

ABSTRACT

We present a 1-D velocity model of the Earth's crust in Paka and Korosi geothermal prospects in the northern Kenya rift valley obtained by solving the coupled hypocentre–velocity inverse problem for 170 local earthquakes recorded at a dense local network. The model is constructed using the VELEST program, which calculates 1-D 'minimum' velocity model from body wave travel times, together with station corrections, which account for deviations from the simple 1-D structure. From the relocation of the events in the new model, The events are located using the softwares seiscomp3 and relocated in the new model using hypoDD to better interpret the distribution of seismicity in the area. An optimal *Vp*/*Vs* ratio of 1.78 was retrieved from the relocated data events. There after the Poisson's ratio is computed from the Vp/Vs. The results obtained here reveal two major crustal layers namely the first layer with a thickness of 10 km and increasing P-wave velocity of 2.63 to 5.94 km/s and the second layer with a thickness of 12 km and an increasing P-wave velocity from 5.94 to 7.08 km/s whose lower interface coincides with a sharp Moho discontinuity. The average value for the Poisson's ratio is 0.29. The average S wave velocities for the crust is 3.75 km/s.

.

1.0 INTRODUCTION

The analysis of regional seismicity to identify and geometrically characterize active fault structures and estimate the present tectonic regime requires an accurate determination of the spatial distribution of the earthquakes. The quality of absolute event locations is controlled by several factors, including network geometry, number of available phases, arrival-time reading accuracy and information about the crustal structure (Pavlis 1986; Gomberg *et al.*1990).

The knowledge of a realistic velocity structure is necessary to prevent artefacts in the location of hypocentres: inappropriate choice of the velocity model can lead to significant distortions and bias in the hypocentre positions, even when using double-difference methods (Michelini & Lomax 2004).

Parametrizing the Earth crust structure as a layered medium is generally appropriate, since the elastic proprieties of the Earth mainly change with depth due to sedimentation, compaction and thermal processes. The importance of finding a reliable, 1-D reference velocity model has been emphasized in many works (e.g. Crosson 1976; Thurber 1983; Kissling *et al.*1995). 1-D velocity models are routinely used in seismic network operations and in seismological studies to estimate earthquake location, focal mechanisms and other seismic source parameters. Layered velocity models are also required by several methods for the calculation of synthetic Green's function, like the widely used discrete wavenumber approach (Bouchon 2003). Finally, 3-D tomographic models are often obtained as perturbations of a 1-D reference model. Tomographic results and resolution estimates strongly depend on the choice of the initial model: inadequate reference models may in fact severely distort the tomographic images or introduce artefacts that lead to misinterpretations of the results (Kissling *et al.*1995).

In regions with strong lateral variations and irregular topographic surface, significant errors or systematic shifts in earthquake locations can be introduced by the use of simplified 1-D velocity parametrization. In some cases, the complexity of geological structures can be only be represented by 3-D velocity models. In many cases, however, one can (partially) account for the velocity lateral variations by including station and/or source terms in the location procedure (Douglas 1967; Pujol 1988; Shearer 1997) or path-dependent calibrations (Zhan *et al.*2011).

In this paper we determine a 1-D velocity model for earthquake location for the Paka and Korosi prospects in the Northern Kenya Rift, a complex area with geological and geophysical evidence of significant lateral variations of the elastic properties of the medium, associated with the major and minor geological structures Fig 1.

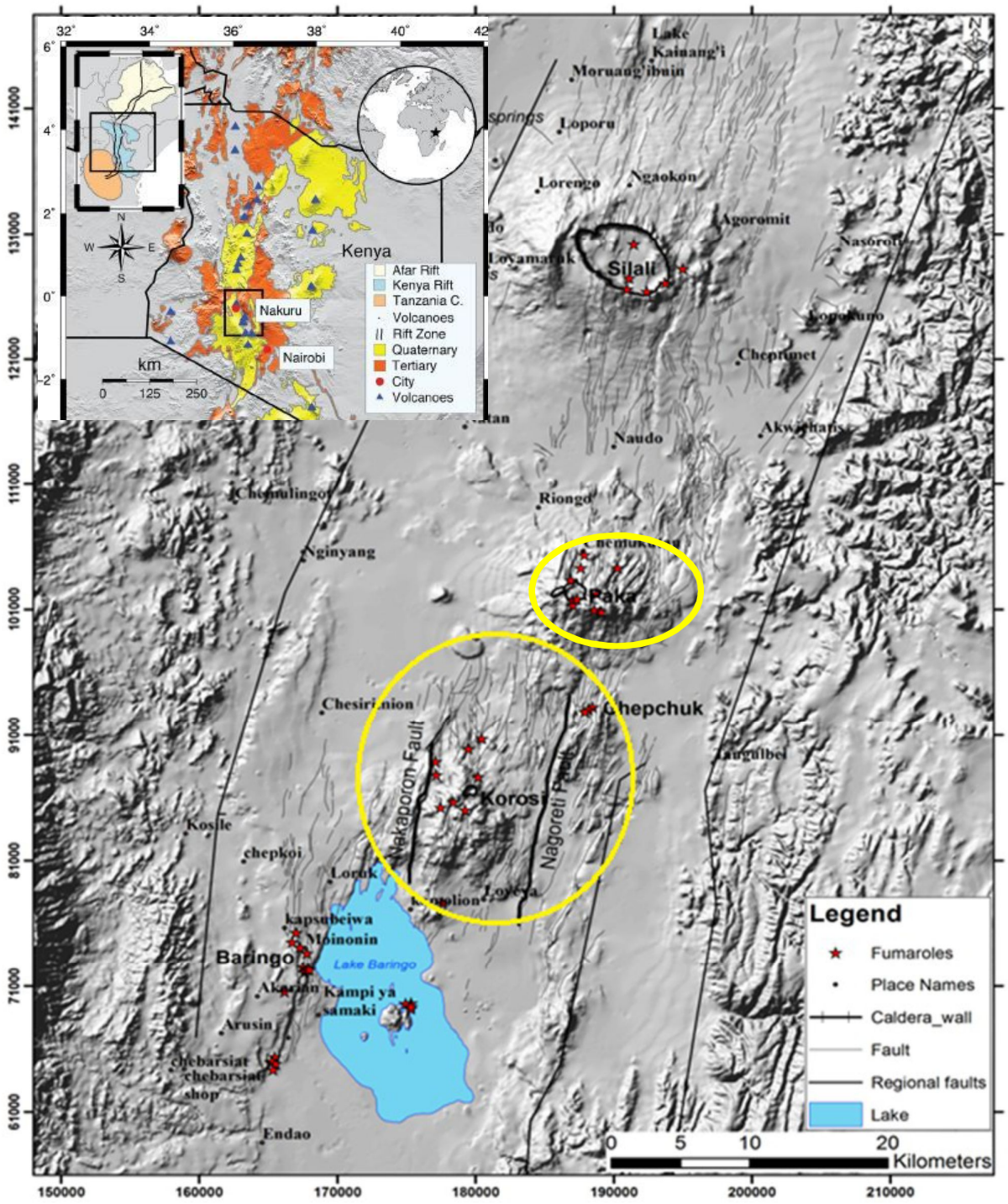

Figure 1: Regional tectonic setting of EARS. In the inset, the bold line shows the rift zone of EARS: colors indicate the individual tectonic rift systems of EARS: Afar rift (yellow), Kenya rift (blue), and Tanzania craton (orange). Main map: yellow and orange represent the Quaternary and Tertiary volcanics, respectively, of the EARS (Patlan et al., 2017). Location of Paka & Korosi geothermal prospect (Yellow circles) on the Kenyan Rift (modified from Lucy Njue,2015).

The Kenyan Rift is an example of active continental rift that is part of the eastern arm of the East African rift zone. Exploration for potential geothermal resources and exploitation has been carried out in the EARS for some time and is still on going. Paka and Korosi volcanic centers being part of the quaternary volcanic centers located along the northern part of the EARS have been the target of a number of recent geoscientific investigations.

The Kenya rift has been known as a region of high geodynamic activity indicated by recent volcanism, geothermal activity and high rate of seismicity. The first micro seismic study in the southern part of the rift was carried out by Molnar & Aggarwal (1971) whose results indicated that seismic activity was located within the rift zone and aligned with regional tectonic faults. The study by Ibs-von Seht et al. (2001) focusing in the Magadi rift found a seismic swarm with approximated b-value of 0.75 indicating a strong crust and tectonic origin .Ibs-von Seht et al. (2001) further derived focal mechanism in the region and found tensional stress field corresponding with Kenya rift. His results were in agreement with studies by Tongue et al., 1994.

Tongue (1991), as part of the Kenya Rift International Seismic Project (KRISP 85 utilized a temporary seismic network near Lake Bogoria. Whereby he investigated the geothermal activity around the southern shores Lake Bogoria. The studies evaluated different sites around the Kenya rift system for decades to understand the volcanic and rift process in the EARS. A study on seismic zone of east Africa by Patlan et al., 2017 identified a volcanic system located in Paka volcano and found a P-axis strike NE-SW for the Paka swarm .The author also applied 3D tomography studies to examine the velocity structure of the upper crust of Paka and korosi whereby he identified a magma chamber at 6km depth beneath paka volcano indicated by seismicity and low s wave velocity suggesting that Paka and korosi are potential for geothermal production.

At present the area is characterized by several seismic swarms (Patlan et al., 2017) and significant low-magnitude ($M_L < 3$) background seismicity that delineates both NE–SW–striking structures. Focal mechanisms at Paka suggest the P-axis is striking NE-SW and are indicative of faulting being controlled by local stresses and tectonic regional stress (Patlan et al., 2017).

A 1-D velocity model available in the literature by Simiyu and Keller (2000) have been used for the study region at different spatial scales; for example the study of Seismic Zone at East Africa Rift: Insights into the Geothermal Potential (patlan et.,al 2017) and for geohazard monitoring studies by geothermal development company (GDC internal reports 2017 and 2018). The model used could have significant differences in *P*-wave velocity values, and in number and depth of interfaces due to the different tools and data used in each study, as well as to the true complexity of the propagation medium.

Starting from 2009, with the deployment of the dense, wide-dynamic range, Seismic Network (GDC: 2009 to date), the capability of detecting and accurately locating small magnitude events ($M_L<3$) in the Paka and korosi prospects has greatly increased. Automatic detection, complemented by manual revision and integration of the event catalogue, has provided a

new, large data set of high-quality phase readings that we used for determining a new reference 1-D model of the region.

In this work, we present this new model, and we illustrate the approach used to determine a robust and reliable 1-D reference structure for the area that takes into account for the actual complexity of the propagation medium through well-defined traveltime station corrections. The data set used consists of 170 events that occurred in the period 2012 August–2018 June and recorded by 10 seismic stations.

2.0. GEOLOGICAL AND GEOPHYSICAL SETTING OF THE INVESTIGATED AREA

The East African rift system is an active continental rift zone. It is a developing divergent plate boundary and therefore accompanied by intense volcanism and volcanic activities. The volcanism activities have been taking place since late tertiary to recent. It is formed by the Somalian and Nubian plates pulling away from the Arabian Plate causing the crustal thinning of the floor of the rift. This tectonic movement started during the early Miocene. It extends from the Afar Triple Junction, which continues south as the Kenyan Rift Valley (Rooney et al., 2014). The Kenyan rift extends from Lake Turkana to northern Tanzania (Figure 1). The formation of the rift started by up doming and volcanism on the crest of uplift and followed by faulting to form a half graben (Roberts et al., 2012; Rooney et al., 2014). The full graben formed during the early Pleistocene, the floor has erupted lava flows of basaltic and trachytic composition, and intercalated with tuffs. The sheet trachytes had dominant north-south closely spaced faults.

A super swell occurred along the East African Rift System (EARS) During the last 40 to 30 million years (Myr) ago resulting in elevated topography, evolving from a complex pattern of mantle circulation and rift plume (Roberts et al., 2012; Rooney et al., 2014). The EARS has significant heat flow, high-elevation (~3000 km), and spreading rate of 2.1 mm/yr., which is attributed to uplift and/or rift initiation (Chorowicz, 2005; Halldòrsson et al., 2014; Simiyu, 2009).

The entire length of the Kenyan rift has shield volcanoes formed during the quaternary period dominantly of silicic composition (Mutonga. 2013). These volcanoes are korosi, Paka, silali, emuruangogolak, Namarunu and barrier. These volcanoes are generally complex multi vent low basalt-trachyte volcano dominated by a young central caldera at the summit (Mutonga. 2013). Northern rift volcanoes have basalts and oligoclase bearing basalts (mugearites) forming bimodal association with trachytes (Williams et al, 1984).

The most recent volcanic activity in the Kenya rift system occurred about 180 years BC (Clarke et al., 1987) The earliest eruption activity at Silali has been estimated to be no more than few hundred years old (Williams et al., 1984). At Paka volcano the most recent eruptions occurred 10 Ka and there is widespread fumarolic activity, and hydrothermally altered rocks

(Simiyu 2010). The composition of the Silali-Paka-Korosi volcanoes show evidence of basalt flows and pyroclastic material (Williams et al., 1984; Simiyu 2010).

3.0 SEISMIC NETWORK, DATA COLLECTION, PROCESSING AND ANALYSIS

Since 2009, the seismic activity in the Paka and Korosi prospect is monitored and operated by GDC with a permanent seismic network, consisting of 10 stations covering an area of 35 km by 25 km, with average interstation distance from 5 to 10 km. Geothermal Development Company (GDC) network was set up in two phases. The first phase comprised of ten seismic stations in Paka, Silali and Korosi geothermal prospect areas. The average station spacing was approximately 10 km between stations. In the second phase, the sensors from Silali were moved to Paka and Korosi prospects for optimization of the network. Data obtained from eight stations in paka and Korosi areas has been analyzed and used in this paper. The network is equipped with 4 three-components broad-band seismometers (Nanometrics Trillium compact)and 4 and one component sensors (Lenartz LE-1DV),allowing for better quality in the determination of the hypocentral parameters.

The equipment are installed close to private homesteads for security purposes and to maximize signal to noise ratio the sensors are buried in a vault one meter below the surface on a bedrock and data is collected manually once every month The location of the seismic stations is shown in Figure 2 and table 1 below.

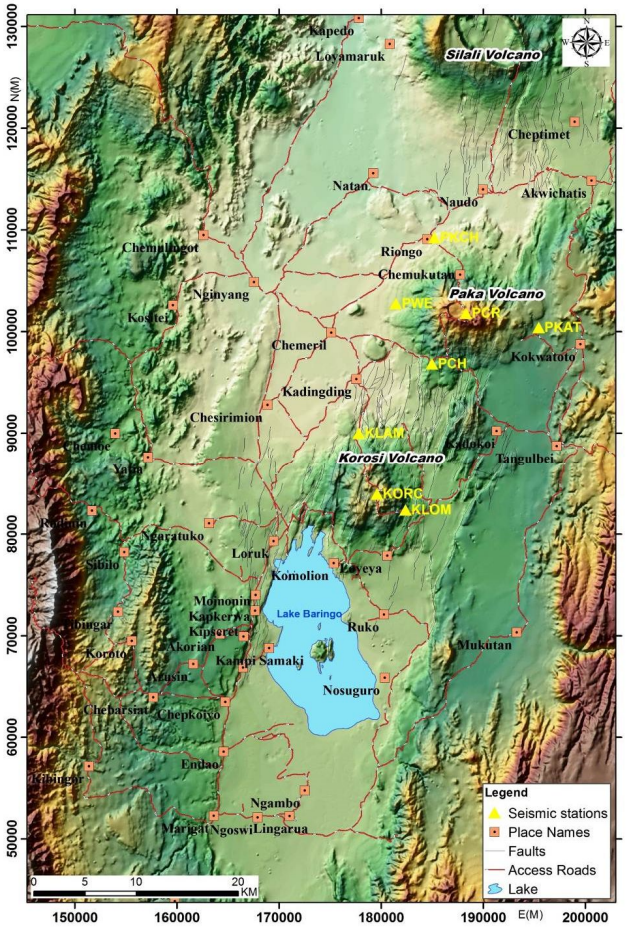

Figure 2: Location of Paka and Korosi Seismic stations from September 2009 to date 2016.

Table 1: Station locations for Paka and Korosi seismic network.

Station Code	Latitude	Longitude	Depth(km)	Type Of Sensor
PCR	0.917667	36.20135	1000	Lenartz LE-1DV
PCH	0.87226	36.171	1118	Lenartz LE-1DV
PWE	0.92571	36.13915	974	Lenartz LE-1DV
PKAT	0.90471	36.26476	1217	Lenartz LE-1DV
PKCH	0.9551	36.19488	1090	Trillium compact
KLOM	0.74453	36.14702	1109	Trillium compact
KORC	0.7587	36.1217	1359	Trillium compact
KLAM	0.813303	36.1059	995	Trillium compact

The data Obtained is in REFTEK format recorded using REFTEK data acquisition system. The reftek format was converted to miniseed format for processing using the seiscomp3

software. The miniseed waveform data was then reviewed using the PQL software to check for data quality and archiving was carried out..

4.0 DATA PRESENTATION, ANALYSIS AND INTERPRETATION

After archiving the data and checking for data quality,SeisComp3 software (Seismological Communication Processor) by GEOPHON was used to perform automatic detections and identify possible arrivals. Several filters and detection parameters were used to search for local events. After automatic detections were made we associated arrivals to possible hypothetical events which were reviewed manually.

The 1D velocity model from Simiyu and Keller (2000) shown in figure 3, is used in the location of the event/earthquakes as the initial model.

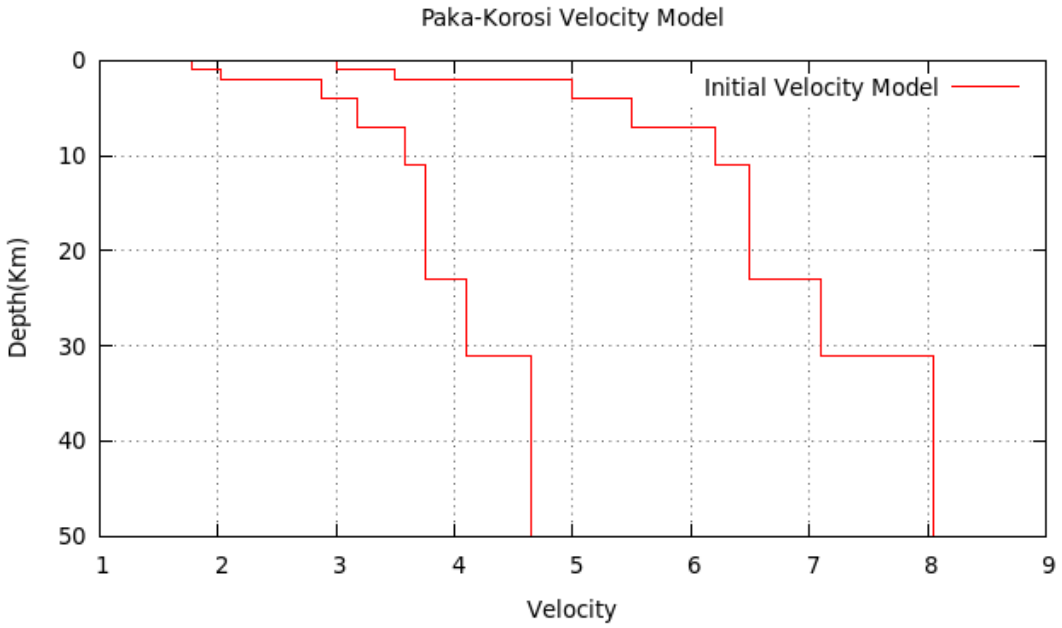

Figure 3: Initial velocity model (Simiyu and Keller. 2000)

The data set used in this study consists 170 small-magnitude earthquakes from GDC network (2012-2018), with local magnitude ranging between 0.1 and 3.2 (Figure.4&5), occurred from 2012 September 2012 to 2018 June. To obtain a high-quality data set, we manually picked the first *P*- and *S*-wave arrival times of earthquakes recorded by at least four stations. A weighting factor was assigned to the readings of the first *P*- and *S*-wave arrival times according to the estimated uncertainties (decreasing weighting factors were associated to uncertainties <0.05 s, 0.05–0.10 s, 0.10–0.20 s, 0.20–0.50 s and >0.50 s).

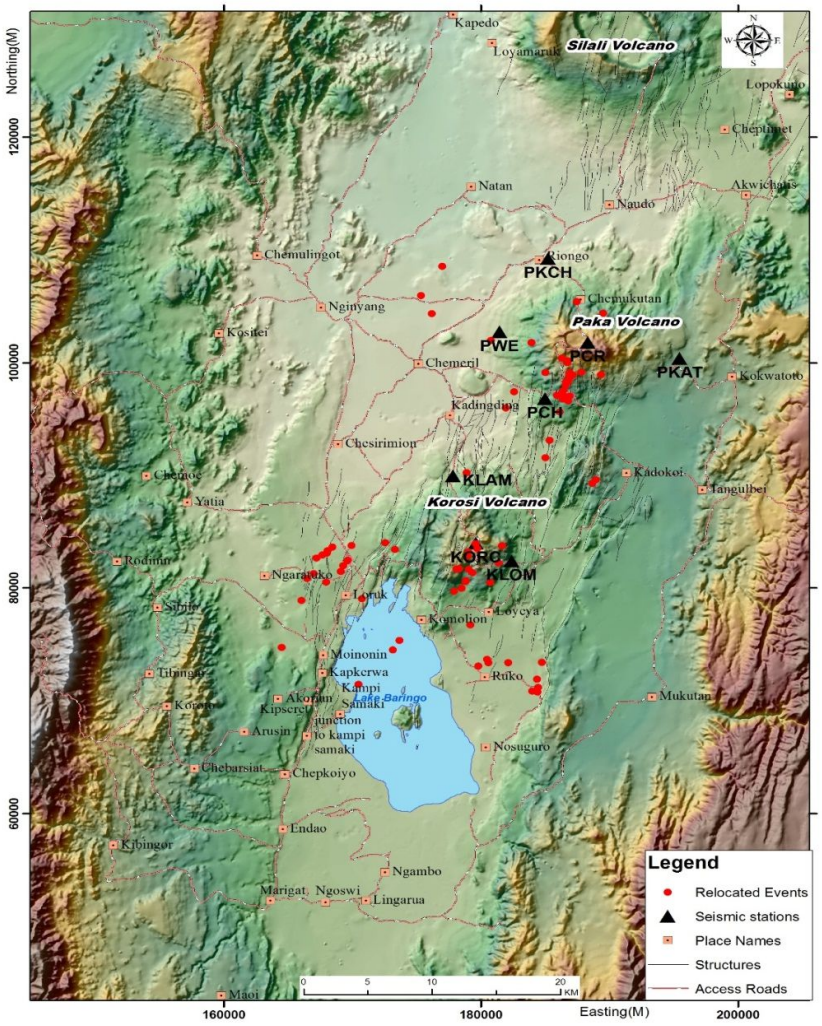

Figure 4: Epicentral map showing routine locations of the studied earthquakes (seiscomp3 events)

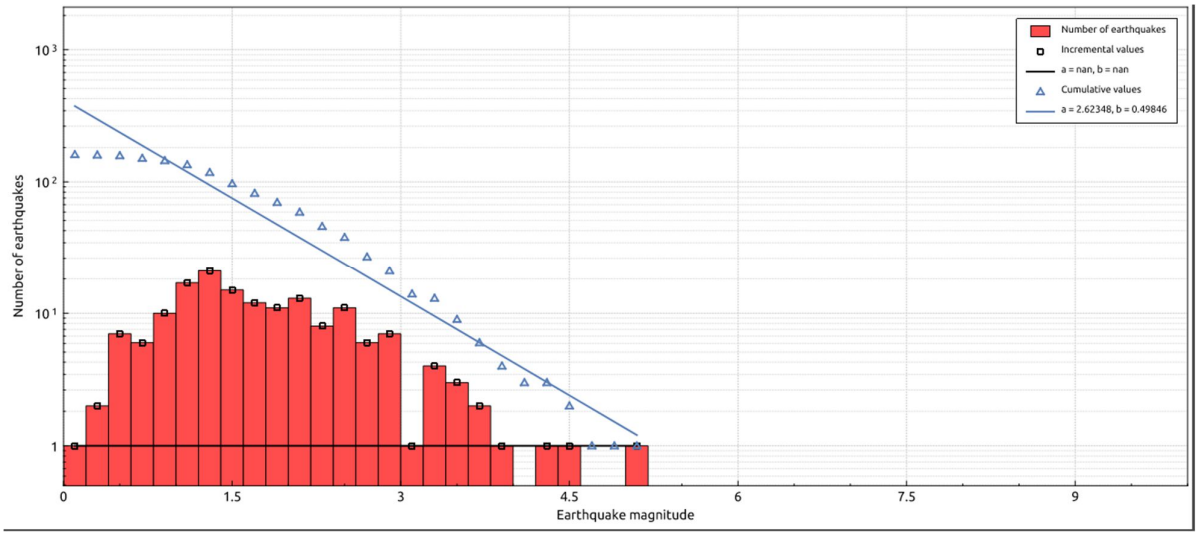

Figure 5: Gutenberg-Richter distribution of relocated earthquakes below the flank of Paka and Korosi volcano the y-axis plot shows the log of the number of events versus earthquake local magnitude.

A first evaluation of picking consistency has been performed by analysing the 'modified Wadati diagram' (Chatelain 1978), which also provides an estimate of the average V_p/V_s ratio. In this diagram, we considered Modified Wadati diagram' showing for each event, the difference between arrival times of *P*-phase and S phases ($Vs - Vp$, y-axis) and *P*-phase ($_{Vp}$, *x*-axis) arrival times. In blue line is the best-fit line (which provides an estimate of an average *Vp*/*Vs* ratio of 1.78 this representation does not depend on the earthquake origin time. The data are well distributed around a linear trend and the least-square best-fit line provides a slope, equal to the *Vp*/*Vs* ratio, of 1.78 with an rms of 0.003 (Figure.6).

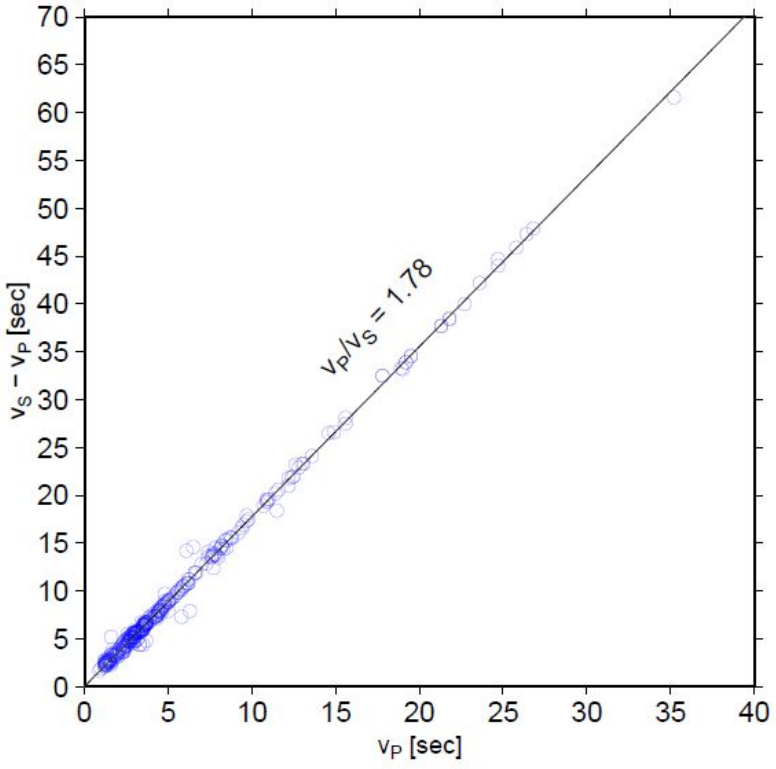

Figure 6: Modified Wadati diagram' showing for each event, the difference between arrival times of P-phase and S phases (Vs − Vp, y-axis) and P-phase (Vp, x-axis) arrival times. In blue line is the best-fit line (which provides an estimate of an average Vp/Vs ratio of 1.78 .Vp/Vs ratio for Paka Korosi data set.

Arrival times that departed significantly from this trend were considered as outliers and therefore identified and removed from the data set. We performed a selection removing picks significantly outside of residuals (>1 s), and the final data set consists of 641-*P* and 287 S-arrival time readings.

4.0 1-D *P*-WAVE VELOCITY MODEL

Seismic wave travel time is a non-linear function of the hypocentral parameters and of the seismic velocities sampled along the ray path between the hypocentre and the station. The bias between the hypocentral parameters and seismic velocity is known as the 'coupled hypocentre–velocity model problem' (Crosson 1976; Kissling 1988; Thurber 1992). In a standard location procedure, the velocity parameters are maintained fixed to *a priori* values and the observed traveltime residuals are minimized by perturbing the four hypo central parameters (origin time, epicentre coordinates and depth). Precise hypocentre locations demand the simultaneous solution of both velocity and hypocentral parameters.

In order to determine the best *P*-wave 1-D velocity model of the study area we used the VELEST code developed by Kissling *et al.* (1995). The non-linear problem is linearized and the solution is obtained iteratively, each iteration consisting in solving both the complete forward problem and the complete inverse problem at once. The inverse problem is solved by inversion of the damped least-square matrix of traveltime partial derivatives. To account for velocity lateral heterogeneities in the subsurface, station corrections are included in the 'minimum 1-D velocity model' inversion. For a more detailed description of VELEST methodology, the reader is referred to Kissling (1995).

VELEST solves for the *S*- and the *P*-wave velocity model independently or jointly. It is suitable for cases in which the ratio N_p/N_s (N_p and N_s being the number of *P* and *S* time readings, respectively) is high and the uncertainties on the *S*-wave readings are comparable with *P* uncertainties. We restricted this study to the V_p model determination since the amount and the quality of *S*-wave arrival times were not sufficiently high to obtain a reliable and accurate V_s model, and we chose to find the best average V_p/V_s ratio considering the *P*-wave velocity models as the reference models.

In the inversion process, we considered only the events with the following features: at least four *P*-arrival time readings, a maximum location error (both horizontal and vertical) of 10 km, and maximum rms of 0.5 s. This refined data set is composed of 641 first *P* arrival time readings and 287 S arrival time readings, corresponding to 170 localized events.

A critical factor for the linearized inverse problem, already stressed by several authors (Kissling 1988; Thurber 1992; Kissling *et al.*1995), is the importance of the initial velocity model that affects the whole process of inversion. Here we tackle this problem by exploring six different 1-D initial V_p models, one of which is taken from literature and the remaining five being simple homogeneous or gradient models. Some additional layers every 1 km were introduced for each considered model, since VELEST does not invert for changes in layer thickness.

Damping factors for the hypocentral parameters, station delays and velocity parameters were selected optimizing the data misfit reduction and the parameters resolution. We chose to avoid low velocity layers so as not to introduce instabilities in the inversion process. For each initial velocity model, the convergence to a stable solution isobtained after 15–20 iterations and the final models (Figure.7) are characterized by rms values ranging between 0.07 and 0.19 s.

We tested the location stability, using VELEST, by shifting the initial hypocenter locations randomly in space before the inversion process. This provides a way to check the bias in the hypocentral locations and the solution stability of the coupled problem. If the retrieved 'Minimum 1-D velocity model' is a robust minimum in the solutions space, there should be no significant changes in the final hypocentral locations. We generated several data sets adding to the initial hypocentre coordinates random noise (±5 km in both vertical and horizontal directions), according to the average error on earthquake location, and we repeated the inversion procedure.

The final locations, obtained starting the inversion process with perturbed earthquakes location, are compared with those obtained starting with the unperturbed locations.

To account for local deviations from the 1-D velocity model, station corrections are computed during the inversion procedure. Positive and negative values of station correction—with respect

to a reference station—correspond to local low- and high-velocity anomalies, respectively, in the vicinity of the recording station. VELEST allows for the use of station elevations during inversion,

and rays are traced to the true station position. This is an important constraint since in the study area, the elevation of the recording sites ranges from 0.974 to 1.359 km a.s.l. Station corrections are computed with respect to a reference station, PCH, whose delay is close to zero. We chose this station because it lies towards the middle of the network, has a large number of readings with a small error on the observation and is located in an area where the surface geology is known.

5.0 RESULTS.

Earthquakes often occur in regions of complex geology, making it difficult to determine their locations due to uncertainty in path effects. Usually a 3-D velocity model can account for most of the traveltime anomalies that are not included in a 1-D model. However, 1-D models are sometimes a necessary—if not preferred—choice, for routine earthquake location, double-difference relocation, source parameter computation, Green's function calculation and as a starting point for 3-D tomographic analyses.

In this work we retrieved a robust and reliable 1-D reference *P*-wave velocity model for a structurally complex area (Paka and Korosi area), from the analysis of background regional seismicity ($M < 3.1$). The procedure involved determining a *P*-wave 'Minimum 1-D velocity model' using VELEST (Kissling *et al.*1995);

The retrieved 'minimum 1-D velocity model' Figure 7 & Table 2 reveal two major crustal layers namely the first layer with a thickness of 10 km and increasing P-wave velocity of 2.63 to 5.94 km/s and The first layer is composed of three minor layers whose depths and velocity values vary from each other. The model is characterized by a $V_p = 2.63$ km s^{-1} shallow layer (down to sea level), whose velocity is consistent with the average *P*-wave velocity value related to the different surface lithologies in the area, which vary from alluvium to the

Western part of the prospects and the upper trachytes sequence to the North Eastern part. The second layer, 1 km thick, with V_p = 3.41 km s^{-1}, is interpreted to be compatible with the depth range of Miocene –Pliocene trachytes and basalts in the area. A transition that occurs gradually passing across a layer of 3 km (V_p = 4.89 km s^{-1}), is observed on the third minor layer whose bottom interface I at a depth of 10km with Vp values of 5.94 km s^{-1} is interpreted to be end of the first major layer. The second layer with a thickness of 12 km and an increasing P-wave velocity from 5.94 to 7.08 km/s is observed at a depth of 10km up to24km whose lower interface coincides with a sharp Moho discontinuity.

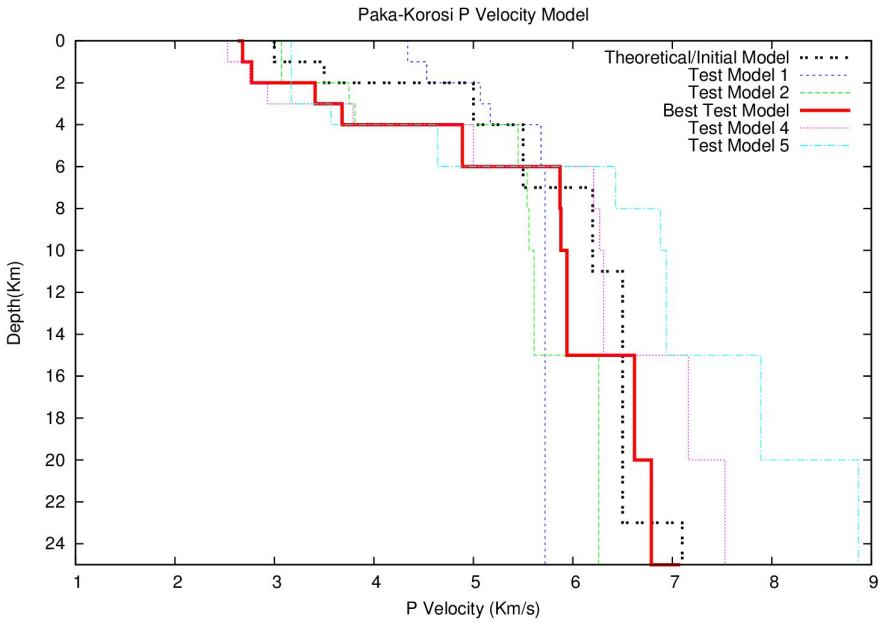

Figure 7: Paka Korosi 'Minimum' 1-D velocity model comparison between the initial model (dotted black and the computed model using VELEST (red).

Table 2. 'Minimum' 1-D velocity model. In the first column are indicated the depth of the top (km)

for each layer. In the second column the *P*-wave .velocity value (km s−1).

Top of Layer km)	Vp (km/s)	Vs (Km/s)	
-3	2.63	0.75	
0	2.68	1.21	
1	2.77	1.88	
2	3.41	2.44	10km thick major layer1
3	3.68	3.02	
4	4.89	3.09	
6	5.87	3.34	
8	5.88	3.53	
10	5.94	3.55	
15	6.62	3.73	12km thick major layer 2
20	6.79	4.02	
25	7.08	4.21	Moho discontinuity

From the relocation of the events in the new model, we were able to retrieve an optimal *Vp*/*Vs* ratio, as the value that minimizes the location rms. We interpret the high *Vp*/*Vs* value of 1.78 to be due to high thermal gradient beneath Paka and Korosi prospect.

As a final step, to better interpret the distribution of seismicity in the area, we further relocated our data set using the double difference technique (HypoDD—Waldhauser & Ellsworth 2000; Waldhauser 2001). Relative locations from double-difference further minimize errors related to un-modelled velocity structures, under the assumption that ray paths from the events to a common station are similar. This assumption is verified, in our case, since hypocentral separation is small compared to the event–station distance and to the length scale of the velocity heterogeneities.

122 earthquakes (from the initial data set consisting of 170 earthquakes) were successfully relocated using HypoDD and their epicentral distribution is shown in figure 8 below. One major seimic swarm was identified and located paka volcanic systems showing a pipe-like pattern of seismicity at the summit of the crater as shown in Figure 9.

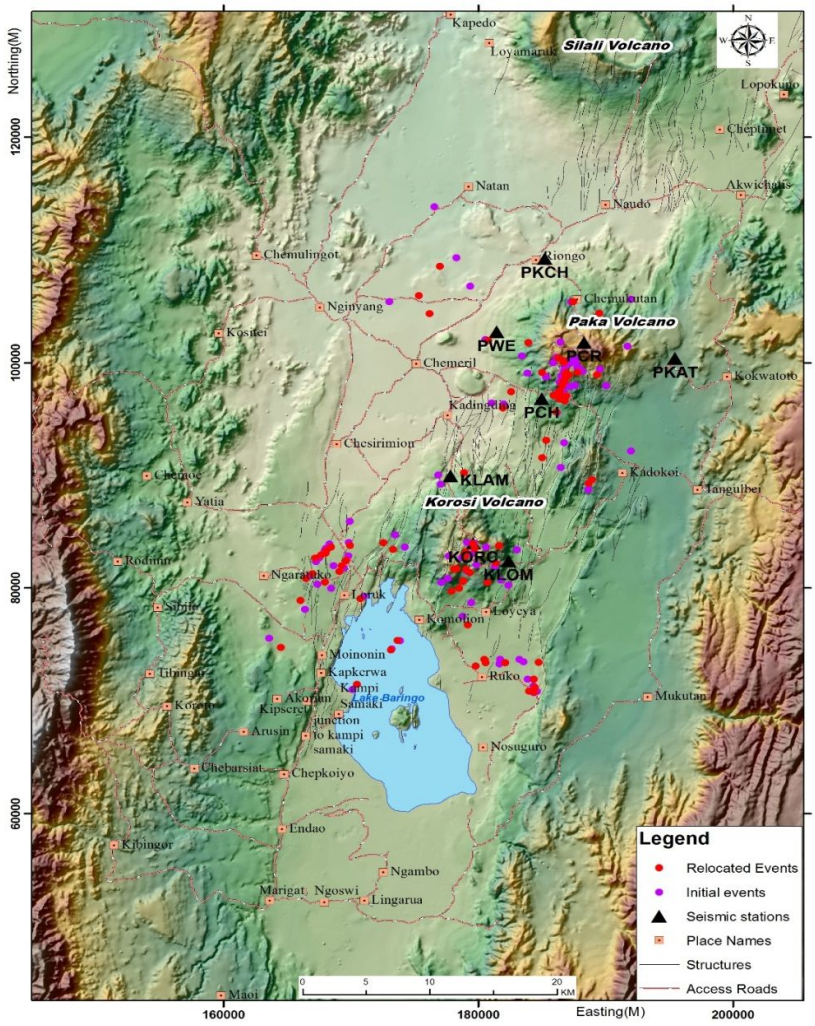

Figure 1: Map view of the seismicity from 2012 September to 2018 June relocated through double-difference method, using the 1-D velocity model obtained in this study.

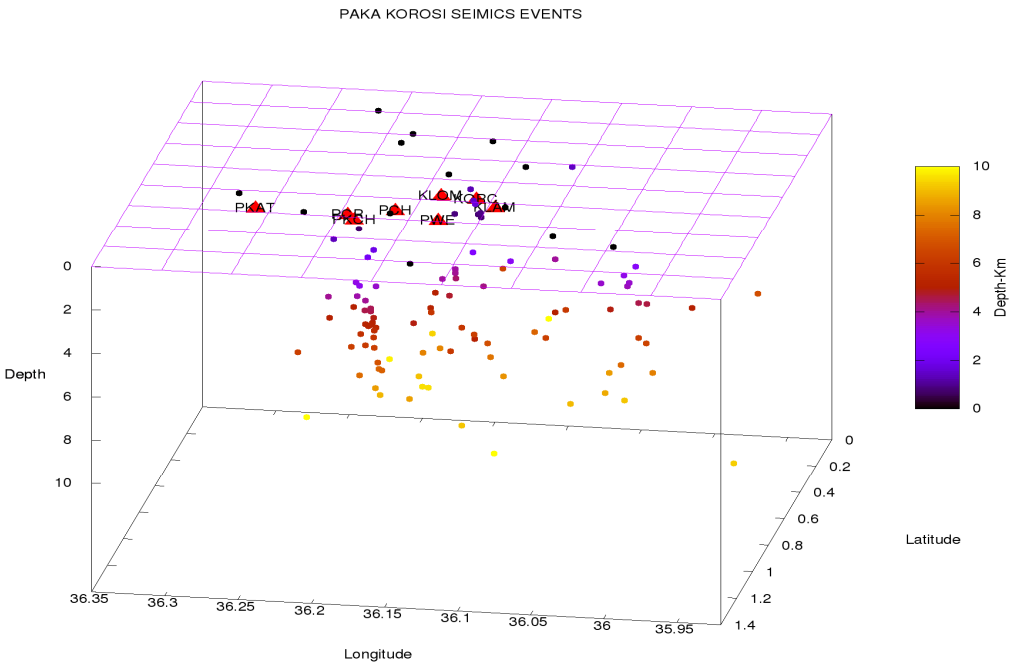

Figure 9: Hypocenters of the 170 earthquakes recorded during (September 2012 to June 2018 deployment) at Paka volcanic center. Ranging depth of 0km to 12km

5.0 DISCUSSION, CONCLUSION AND RECOMMENDATIONS

The crustal velocity model derived from the micro earthquakes data is consistent with a 10 km upper crust and a 12 km lower crust.

Results reveal two major crustal layers; the first layer with a thickness of 10 km and increasing P-wave velocity of 2.63 to 5.94 km/s and the second layer with a thickness of 12 km and an increasing P-wave velocity from 5.94 to 7.08 km/s whose lower interface coincides with a sharp Moho discontinuity. The average value for the Poisson's ratio is 0.29. The average S-wave velocity for the crust average is 3.75 km/s.

One major seismic swarm was identified and located paka volcanic systems showing a pipe-like pattern of seismicity at the summit of the crater.

Combining structural geology analysis with relocated seismic events provides a high-confidence approach to structural correlation and mapping of micro seismic events. It is observed that there is a strong relationship between the location of events and surface geological structures such as faults and lineaments. Paka prospect is highly fractured and

majority of events are located around the areas with major and minor fractures and faults. The e seismic activity observed in the two prospects could be related to high thermal gradient in the region and fluid movement within the region .

To conclude, a reference 1-D velocity model for the Paka and Korosi geothermal prospects was a necessary requirement for current routine operations at the Geothermal development Company (GDC network) and for future refined seismological studies. We introduced a robust and reliable model obtained by careful selection and repicking of 170 small-magnitude earthquakes. An independent strategy to check location quality seems therefore to be a required step when deriving 'minimum 1-D models'. Validation, through the comparison with a 3-D tomographic model to check if a significant bias can exist between earthquake locations and station corrections, leading to systematic shifts in hypocentral positions is recommended.

REFERENCES

REFERENCES

Bouchon, M..Areviewof the discretewavenumber method, in *Seismic Motion, Lithospheric Structures, Earthquake and Volcanic Sources: The Keiiti Aki Volume,* Pageoph Topical Volumes 2003, pp. 445–465.

Chorowicz J.The east African rift system, Elsevier: Journal of African Earth Sciences(2005), 43, 379-410.

Clarke, M.C.G., D.G. Woodhall, (1987), Geological and geothermal mapping. British Survey, Exploration for Geothermal Energy Project, Progress report BGSKEN/2, 135 pp.

Clarke, M.C.G.,and D.G. Woodhall.Geological and geothermal mapping. British Survey, Exploration for Geothermal Energy Project, Progress report (1987), BGSKEN/2, 135 pp.

Crosson, R.S. Crustal structure modelling of earthquake data.Simultaneous least squares estimation of hypocentre and velocity parameters,*J. geophys.* 1976 *Res,* 81, 3036–3046.

Crosson, R.S., 1976. Crustal structure modelling of earthquake data. Simultaneous least squares estimation of hypocentre and velocity parameters,*J. geophys. Res,* 81, 3036–3046.

Douglas, A. 1967. Joint epicentre determination, *Nature,* **215,** 47–48.Ekstrom, G., 1994. Teleseismic analysis of the 1990 and 1991 earthquakes near Potenza, *Ann. Geofis.,* **XXXVII,** 1591–1599.

Dunkley, P. N., Smith, M., Allen, D. J., & Darling, W. G. The geothermal activity and geology of the northern sector of the Kenya Rift Valley. (1993).

E. Patlan, Velasco, A., G. Kaip, A. Wamalwa.Seismic Zone at East Africa Rift: Insights into the Geothermal Potential PROCEEDINGS, 42nd Workshop on Geothermal Reservoir Engineering Stanford University, Stanford, California, February 13-15, 2017 SGP-TR-212.

Gomberg, J.S., Shedlock, K.M. & Roecke, S.W. The effect of S-wave arrival times on the accuracy of hypocenter estimation, 1990 *Bull. seism. Soc.Am.,* **80,** 1605–1628

Gutenberg, B., and C. F. Richter.Frequency of earthquakes in California, *Bulletin of the Seismological Society of America*, 194, *34*(4), 185–188.

Halld´orsson, S. A., D. R. Hilton, P. Scarsi, T. Abebe, and J. Hopp .A common mantle plume source beneath the entire East African Rift System re- vealed by coupled helium-neon systematics, *Geophys. Res. Lett.*, *41*, 2304-2311, doi: 10.1002/2014GL059424. (2014).

Hemming.Initiation of the western branch of the East African Rift coeval with the eastern branch, 2012, Nature Geoscience, 5,289-294

Ibs-von Seht, M., S. Blumenstein, R. Wagner, D. Hollnack, and J. Wohlenberg .Seismicity, seismotectonics and crustal structure of the southern Kenya Rift—new data from the Lake Magadi area, 2001, *Geophysical Journal International*, *146*(2), 439–453.

Keller, G. R., M. A. Khan, P. Morganc, R. F. Wendlandt, W. S. Baldridge, K. H. Olsen, C. Prodehl, and L. W. Braile .A comparative study of the Rio Grande and Kenya rifts, *Tectonophysics*, 1991, *197*(2), 355–371.

Kennett, B. L. N., and E. R. Engdahl.Traveltimes for global earthquake location and phase identification. Geophysical Journal International, 1991 122, 429–465.

Kim, K., A. A. Nyblade, J. Rhie, C. Baag, and T.S. Kang (2012), Crustal S-wave velocity structure of the Main Ethiopian Rift from ambient noise tomography, Geophysical Journal International, 191, 865-878.

Kissling, E., 1995. *Velest User's Guide. Internal Report,* 26 pp., Institute ofGeophysics, ETH Zurich.

Kissling, E., Ellsworth, W.L., Eberhart-Phillips, D. & Kradolfer, U., 1995.Initial reference models in local earthquake tomography, *J. geophys. Res.,* **99,** 19 635–19 646.

Kissling, E., Geotomography with local earthquake data Rev. Geophysics1988, 26,659-698.

Kissling, E., Geotomography with local earthquake data, (1988) *Rev.Geophys.,* **26,** 659–698.

Mechie, J., Keller, G.R., Prodehl, C., Khan, M.A., and Gaciri, S.J., 1997, Structure and dynamic processes in the lithosphere of the Afro-Arabian Rift system: A model for the structure, composition and evolution of the Kenya Rift: Tectonophysics, v. 278, p. 95–119.

Michelini, A. & Lomax, A.The effect of velocity structure errors on double-difference earthquake location, *Geophys. Res. Lett.*, 2004. **31,** L09602, doi:10.1029/2004GL019682.

Molnar, P., and Y. P. Aggarwal.A microearthquake survey in Kenya, *Bulletin of the Seismological Society of America*,1971 *61*(1),

Molnar, P., and Y. P. Aggarwal (1971), A microearthquake survey in Kenya, *Bulletin of the Seismological Society of America*, *61*(1), 195–201.

Mutonga, M. The Geology of Paka Volcano, and its Implication on Geothermal. *Geothermal Resources Council Transactions*, (2013). 431-436.

Njue, L.M. Geological Model of Korosi Geothermal Prospect, Kenya Proceedings of the World Geothermal Congress 2015, Melbourne, Australia.

Pavlis, G.L.. Appraising earthquake hypocenter location errors: a complete, practical approach for single event locations, *Bull. seism. Soc. Am.,* 1986 **76,** 1699–1717

Pujol, J. Comments on the joint determination of hypocenter and station corrections, *Bull. seism. Soc. Am.,1988* **78,** 1179–1189.

Roberts, E. M., N. J. Stevens, P. M. O'Connor, P. H. G. M. Dirks, M. D. Gottfried, W. C. Clyde, R. A. Armstrong, A. I. S. Kemp, S.Hemming .Initiation of the western branch of the East African Rift coeval with the eastern branch, Nature Geoscience, 2012, 5,289-294.

Roberts, E. M., Stevens, N. J., O'Connor, P. M., Dirks, P. H. G. M., Gottfried, M. D., Clyde, W. C.,& Hemming, S. Initiation of the western branch of the East African Rift coeval with the eastern branch. *Nature Geoscience*, 2012. *5*(4), 289.

Rooney, T. O., I. D. Bastow, D. Keir, F. Mazzarini, E. Movsesian, E. B. Grosfils, J. R. Zimbelman, G. Yirgu The protracted development of focused magmatic intrusion during Continental rifting: focused magma intrusion during rifting, Tectonics, (2014), 33(6), 875–897,doi:10.1002/2013TC003514.

Rooney, T. O., I. D. Bastow, D. Keir, F. Mazzarini, E. Movsesian, E. B. Grosfils, J. R. Zimbelman, M. S. Ramsey, D. Ayalew, and G.Yirgu (2014), The protracted development of focused magmatic intrusion during continental rifting: focused magma intrusion during rifting, *Tectonics*, *33*(6), 875–897, doi:10.1002/2013TC003514.

Sceal, J. C.,The Geology of Paka volcano and the country east, Baringo District (1974).

Shearer, P.M., 1997. Improving local earthquake locations using the L1 norm andwaveformcorrelation application to the Whittier Narrows, California, aftershock sequence, *J. geophys. Res.,* **102**(B4), 8269–8283.

Simiyu, S., and G. R. Keller, (2001), An integrated geophysical analysis of the upper crust of the southern Kenya rift. *Geophysical Journal International*. 147: 543-561.

Simiyu, S., Application of micro-seismic methods to geothermal exploration: examples from the Kenyan rift, *United Nations University and LaGeo*, **1**, (2009), 1-27

Thurber, C.H., 1983. Earthquake locations and three-dimensional crustal structure in the Coyote Lake Area, Central California, *J. geophys. Res.,* **88**(B10), 8226–8236.

Thurber, CH., 1992. Hypocentre–velocity structure coupling in local earthquake tomography, *Phys. Earth planet. Inter.,* **75,** 55–62

Tongue, J. A. Tomographic study of local earthquake data from the Lake Bogoria region of the Kenya Rift Valley, *Geophysical Journal International*,1992 *109*(2), 249–258.

Tongue, J., P. Maguire, and P. Burton 1994, An earthquake study in the Lake Baringo basin of the central Kenya Rift, *Tectonophysics*,1994, *236*(1–4), 151–164.

Waldhauser, F. & Ellsworth, W.L.. A double-difference earthquake location algorithm: method and application to the northern Hayward Fault, California, *Bull. seism. Soc.* 2000 *Am,* **90,** 1353–1368.

Waldhauser, F.. hypoDD: A computer program to compute doubledifference hypocenter locations. Open File Rep, U.S. Geol. Surv. 2001, 01–113.

Waldhauser, F., and W. L. Ellsworth A double-difference earthquake location algorithm: Method and application to the northern Hayward fault, California, *Bulletin of the Seismological Society of America*,2000 *90*(6), 1353–1368.

Wang, C.T., and Horne, R.N. "Boiling Flow in a Horizontal Fracture." *Geothermics*, 29, (1999), 759-772.

Williams, L. A. J., Macdonald, R., & Chapman, G. R., Late Quaternary caldera volcanoes of the Kenya Rift valley. *Journal of Geophysical Research: Solid Earth*,1984, *89*(B10), 8553-8570., Kenya. Unpublished PhD thesis, University of London

Zhan, Z., Wei, S., Ni, S. & Helmberger, D. Earthquake centroid locations using calibration from ambient seismic noise, *Bull. seism. Soc. Am.,* 2011, **101**(3), 1438–1445.